OTC 5006

The Prediction of Lockin Vibration on Flexible Cylinders in a Sheared Flow

by J.K. Vandiver, *Massachusetts Inst. of Technology*

Abstract

A method is proposed for the prediction of the flow induced vibration response of flexible cylinders such as cables, pipes, and risers, in a sheared flow. The significance of material and hydrodynamic sources of damping is discussed. The reduced damping or response parameter plays a key role in response prediction. However, the dependence of the response parameter and therefore the response amplitude on the ratio of cylinder mass per unit length to the displaced fluid mass per unit length is shown to be widely misunderstood. Under lockin conditions, damping is important in determining response amplitude, but cylinder mass per unit length is not.

Introduction

Flexible cylinders, such as cables, drill pipe, and marine risers, often exhibit an harmonic flow induced vibration response known as lockin. Under uniform flow conditions, lockin has been extensively studied and empirical response prediction techniques are often adequate. However, real ocean applications often require response prediction under non-uniform (sheared) flow conditions. Very long cylinders with closely spaced natural frequencies rarely exhibit lockin behavior and frequently behave as infinite strings (1). For shorter cylinders, with well separated natural frequencies, lockin with one mode is possible, even in the presence of shear. However, in such cases, response amplitude is very difficult to predict and it is often difficult to determine which mode, if any, will dominate the response. In this paper, a method for predicting lockin in a sheared flow is proposed. The method makes extensive use of the concept of the response parameter or reduced damping, as it is sometimes called.

A very common misconception regarding the response parameter is pointed out. The response parameter is shown to be primarily a function of damping and is specifically not a function of the cylinder mass per unit length.

References and figures at end of paper.

Normal Mode Model of Lockin Vibrations

A pipe or cable under tension has, from an analytical view, an infinity of natural modes. When the cylinder is deployed with its longitudinal axis normal to an incident uniform flow, vibration is caused by the shedding of vortices in the wake of the cylinder. The vortex shedding process generates both fluctuating lift and drag forces on the cylinder. Under the correct circumstances, described extensively in the literature, (2,3) a phenomena known as lockin may occur. Lockin is characterized by the synchronization of the wake with either the cross-flow (lift direction) oscillations or with the in-line (drag direction) vibrations. This paper focuses on cross-flow lockin only, in which one cross flow mode dominates the response. At lockin in a uniform flow the lift forces are coherent over the entire length of the cylinder. A normal mode solution to the partial differential equation of motion may be obtained, and is briefly reviewed below.

Consider a beam or string under tension with fixed ends as defined in Figure 1. Let the vortex-induced cross-flow displacement be given by

$$y(x,t) = \sum_i q_i(t)\Psi_i(x) \qquad (1)$$

where the $\Psi_i(x)$ are the mode shapes and the $q_i(t)$ are the modal amplitudes. Using the method of normal mode superposition, and assuming insignificant damping related intermodal coupling, a set of independent equations of motion are obtained, one for each mode. These equations are of the form:

$$M_i\ddot{q}_i + R_i\dot{q}_i + K_iq_i = N_i(t) \qquad (2)$$

This equation is simply that of a linear, single degree of freedom mass-spring-dashpot system excited by a force $N_i(t)$, known as the modal exciting force for mode i. There exists one such

equivalent oscillator for each mode of interest. M_i, R_i, and K_i are known respectively as the modal mass, damping and stiffness. The ratio of K_i to M_i yields the undamped natural frequency for the mode.

$$\omega_i = \sqrt{K_i/M_i} \tag{3}$$

M_i and R_i are given by the following equations:

$$M_i = \int_0^L m(x)\psi_i^2(x)dx \tag{4}$$

$$R_i = \int_0^L r(x)\psi_i^2(x)dx \tag{5}$$

where m(x) and r(x) are the mass per unit length and equivalent linear damping coefficient per unit length. m(x) includes the added mass of fluid and r(x) has units of force per unit velocity per unit length.

The damping ratio for mode i is given by

$$\zeta_i = \frac{R_i}{2\omega_i M_i} \tag{6}$$

If one specifies an harmonic input and assumes an harmonic output of the following forms

$$N_i(t) = |N_i| e^{i\omega t} \tag{7}$$

$$q_i(t) = |q_i| e^{i(\omega t-\phi)} \tag{8}$$

then a solution for the magnitude of the response per unit input force and the phase between the force and the response may be directly obtained.

$$\frac{|q_i|}{|N_i|} = |H_i(\omega)| = \frac{1/K_i}{[(1-\frac{\omega^2}{\omega_i^2})^2+(2\zeta_i\frac{\omega}{\omega_i})^2]^{1/2}} \tag{9}$$

$$\phi = \tan^{-1}\left[\frac{2\zeta_i\omega/\omega_i}{(1-\frac{\omega^2}{\omega_i^2})}\right] \tag{10}$$

$H_i(\omega)$ is known as the frequency function or the response amplitude operator (RAO).

At resonance, the frequency of the external excitation is equal to one of the natural frequencies of the system, indicated here as ω_i. If the corresponding modal damping ratio is small then the response of this mode will dominate the response of all other non-resonant modes. This is the case under cross-flow lockin conditions in a uniform flow. Therefore, it is appropriate to model the cross-flow, resonant lockin response in terms of the normal mode equivalent single degree of freedom system reviewed above.

At resonance, the magnitude and phase of the response reduce to

$$\phi_i = \pi/2 \tag{11}$$

$$|H_i(\omega_i)| = \frac{1}{2\zeta_i K_i} \tag{12}$$

Therefore, the response magnitude is

$$|q_i| = \frac{|N_i|}{K_i} \cdot \frac{1}{2\zeta_i} \tag{13}$$

The term N_i/K_i is the static deflection of the oscillator in response to a constant force N_i, and the term $1/2\zeta_i$ is the dynamic amplification factor due to the resonance. Invoking the definition of the damping ratio, ζ_i, from Equation 6, this response expression can be rewritten as:

$$|q_i| = \frac{|N_i|}{\omega_i R_i} \tag{14}$$

This expression will be of considerable use in the next section, on the interpretation of the response parameter. Henceforth, all discussion will pertain to the response of a single mode.

Understanding the Response Parameter, $S_G = \zeta_s/\mu$

Due to a natural evolution in the understanding of the factors which determine lockin response behavior, over the years this critical parameter has been expressed in many forms, reviewed below.

Response parameter:

$$S_G = \zeta_s/\mu = 2\pi S_t^2 k_s \tag{15}$$

Structural damping ratio:

$$\zeta_s = \frac{\delta_s}{2\pi} = \frac{R_i}{2\omega_i M_i} \tag{16}$$

Mass ratio:

$$\mu = \frac{\rho D^2}{8\pi^2 S_t^2 m} \tag{17}$$

Reduced damping:

$$k_s = \frac{2m\delta_s}{\rho D^2} = \frac{4\pi m\zeta_s}{\rho D^2} \tag{18}$$

Response parameter

$$S_G = \frac{8\pi^2 S_t^2 m\zeta_s}{\rho D^2} \tag{19}$$

ζ_s is the damping ratio due to structural dissipation of energy only, and does not include hydrodynamic sources of damping. δ_s is the associated logarithmic decrement. μ is proportional to the ratio of the displaced fluid mass per unit length $\pi\rho D^2/4$ to the mass (including added mass) per unit length of the cylinder, m.

For cylinders that do not have a constant mass per unit length, the m in these equations is replaced with an equivalent uniform mass per unit length m_e. m_e is the equivalent constant mass per unit length which would yield the same modal mass from Equation 4 as the actual variable mass per unit length m(x). Therefore

$$m_e = \frac{\int_0^L m(x)\Psi_i^2(x)dx}{\int_0^L \Psi_i^2(x)dx} \quad (20)$$

For the remainder of this paper, a constant mass per unit length m shall be assumed, to simplify the analysis.

D is the cylinder diameter, assumed constant, and S_t is the Strouhal number given by

$$S_t = \frac{f_s D}{U} \quad (21)$$

where f_s is the vortex shedding frequency and U is the free stream fluid velocity. At lockin the natural frequency and the vortex shedding frequency are assumed to be equal.

$$2\pi f_s = \omega_s = \omega_i = 2\pi S_t U/D \quad (22)$$

Over many years the variety of these evolved forms has led to confusion and misinterpretation of the significance of the various terms which form the response parameter S_G.

The most serious misinterpretation is the implication that lockin response amplitude depends on the mass ratio, μ. It has been generally believed that very dense cylinders respond with lower amplitudes than low density ones. This is not true. It is in fact dependent on fluid exciting forces and structural damping (not damping ratio). The mass per unit length of the cylinder is only important in determining the natural frequency. The validity of these statements can be demonstrated by simply drawing upon definitions, as shown below.

From Equations 18 and 6

$$k_s = \frac{4\pi m_e \zeta_s}{\rho D^2} = \frac{4\pi m_e R_i}{\rho D^2 2\omega_i M_i} \quad (23)$$

Using the definitions of modal mass, and effective mass per unit length from Equations 4 and 20 yields,

$$k_s = \frac{2\pi R_i}{\rho D^2 \omega_i \int_0^L \Psi_i^2(x)dx} \quad (24)$$

For the case of constant damping constant per unit length, r(x)=r

$$k_s = \frac{2\pi r}{\rho D^2 \omega_i} \quad (25)$$

If k_s is not a function of m(x) then from Equation 15 neither is S_G.

$$S_G = 2\pi S_t^2 k_s \quad (15)$$

$$S_G = \frac{4\pi^2 S_t^2 R_i}{\rho D^2 \omega_i \int_0^L \Psi_i^2(x)dx} \quad (26)$$

R_i is the equivalent, linear, structural modal damping. The actual source of damping may not in fact be linear. For most interesting vibration cases the damping is low and for any specific steady state response amplitude an equivalent linear damping is an acceptable approximation.

There is experimental confirmation that S_G and hence the predicted response do not depend specifically on the mass ratio but on the ratio ζ_s/μ. As shown, this is because in taking this ratio the dependence on mass per unit length cancels out. Griffin in reference (7) presents a plot of response amplitude, $2\bar{Y}/D$, versus reduced velocity $V_r=U/f_nD$ where f_n is the natural frequency. This figure is reproduced in figure 4.

Two different cases are shown, one in air and one in water. For both the ratio ζ_s/μ is approximately constant. However, the damping ratios and therefore the mass ratios are different by an order of magnitude. Bothelo has also observed this apparent lack of specific dependence on μ (8).

Both Griffin and Botelho have pointed out another interesting fact, which can be seen in Figure 4. The in water case has a larger damping ratio, by a factor of 10, and therefore it has a much broader bandwidth, than the in air case with lower damping. The halfpower bandwidth for a linear oscillator is equal to $2\zeta_i\omega_i$. Thus one would expect to see a wider region of large amplitude response in a figure such as 4, for those cylinders with larger damping ratios. This author is of the opinion that the consequence of a higher damping ratio is to make lockin vibration of the cylinder less sensitive to local variations in flow velocity (hence reduced velocity) and therefore more tolerant of shear. In other words, two geometrically similar cables with the same reduced damping but different damping ratios will respond differently to a shear. The one with the higher damping ratio will likely experience lockin over a greater portion of its length.

For most engineers S_G has little physical meaning. In the next section, an attempt is made to clarify it.

An Interpretation of S_G, The Response Parameter

No one denies its importance but a common sense interpretation is needed for S_G. To develop one requires a statement of the equation of motion for the normal mode excited at resonance during lockin. At lockin the lift force per unit length in phase with the cross-flow velocity of the cylinder can be expressed as

$$f(x,t) = 1/2\ \rho U^2 D C_L(x) e^{i\omega_i t} \quad (27)$$

The modal exciting force is given by

$$N_i(t) = \int_0^L f(x,t)\Psi_i(x)dx \quad (28)$$

$$= 1/2\rho U^2 D \int_0^L C_L(x)\Psi_i(x)dx e^{i\omega_i t} \quad (29)$$

Using the expression in Equation 29 for the modal exciting force, the non-linear feedback mechanisms which control response amplitude have been replaced with an equivalent linear exciting force in phase with the velocity of the cylinder. Implicit in this expression are the following assumptions:

i. The lift coefficient $C_L(x)$ must be chosen to yield the response amplitude which would be observed in an experiment and can be estimated from compiled data of S_G versus response amplitude, Figure 2.

ii. Lockin exists over the entire cylinder length.

iii. The modal damping on the left hand side arises from non-hydrodynamic sources only. This is because $C_L(x)$ is a lift coefficient which reflects the net fluid dynamic force on the cylinder. It is in fact the difference between lift force in phase with the velocity of the cylinder due to circulation, and fluid resistive forces due to pressure drag and friction drag opposing the cross-flow velocity of the cylinder. In an experimental sense the net lift force is the only measurable quantity and is therefore used here. Under shear conditions, lockin over a portion of the length is likely. Outside of the lockin region fluid drag forces will have to be estimated and used to modify the estimate of R_i. This will be addressed in the section on response predicton in sheared flow.

iv. Fluid forces in phase with the displacement and acceleration also exist. They are assumed to affect only the fluid added mass of the cylinder and are included in the expression for the modal mass, M_i.

Let the integral shown below be defined as P_u, where the u refers to the uniform flow case,

$$P_u = \int_0^L C_L(x)\ \Psi_i(x)dx \quad (30)$$

Recalling Equation 14, an expression for the modal response amplitude at resonant lockin can be found

$$|q_i| = \frac{|N_i|}{\omega_i R_i} = \frac{\frac{1}{2}\rho D U^2}{\omega_i R_i} P_u \quad (31)$$

From Equation 1 the response magnitude of the entire cylinder to the one resonant mode is

$$y(x) = |q_i|\Psi_i(x) \quad (32)$$

which, when expressed as a double amplitude in diameters peak to peak, can be written as

$$\frac{2y(x)}{D} = \frac{2|q_i|\ \Psi_i(x)}{D} \quad (33)$$

Substitution for $|q_i|$ from Equation 31 leads to

$$\frac{2y(x)}{D} = \frac{2|N_i|\ \Psi_i(x)}{D\omega_i R_i} \quad (34)$$

$$= \frac{\rho U^2 \Psi_i(x) P_u}{\omega_i R_i} \quad (35)$$

Recalling that

$$U = \frac{\omega_i D}{2\pi S_t} \quad (23)$$

and the expression for S_G in Equation 26, leads to:

$$\frac{2y(x)}{D} = \frac{P_u \Psi_i(x)}{S_G \int_0^L \Psi_i^2(x)dx} \quad (36)$$

The maximum response occurs at the maximum value of the mode shape and therefore

$$\frac{2y_{max}}{D} = \frac{P_u \Psi_{i,max}}{S_G \int_0^L \Psi_i^2(x)dx} \quad (37)$$

Therefore, S_G is a dimensionless group which is an integral part of the expression one finds for a prediction of response amplitude, and therefore an experimentally observed dependence of response on S_G should not be surprising.

Griffin (2,4) has compiled and published data relating S_G to observed response. These data are given in Figure 2 and represent the results of many different types of experiments, including cantilevers, spring mounted cylinders, pivoted cylinders and cables. The horizontal axis is S_G and the vertical axis is

$$\frac{2y_{max}\ I_i^{\frac{1}{2}}}{D\Psi_{i,max}} \quad (38)$$

where

$$I_i = \frac{\int_0^L \Psi_i^4(x)\,dx}{\int_0^L \Psi_i^2(x)\,dx} \quad (39)$$

For example, a string or a beam with pinned ends and constant tension have mode shapes which are given by

$$\Psi_i(x) = \sin\left(\frac{i\pi x}{L}\right) \quad (40)$$

and $I_i = 3/4$ (41)

Other values for I_i corresponding to different mode shapes are given in Reference 4, as is a table identifying the source of the data used in Figure 2.

The factor $I_i^{1/2}/\Psi_{imax}$ was used in an attempt to reduce the scatter in plotting response data for many different types of structures versus S_G. That this was the appropriate factor to use to accomodate various mode shapes was based on the assumption that the wake oscillator model correctly predicts response. Implicit in the wake oscillator model are particular assumptions regarding the spatial variation of $C_L(x)$. This author is of the opinion that such models are only approximations and that much of the scatter in the data is due to the fact that the correction factor has substantial error for some types of mode shapes.

It should also be noted that only very little of the data shown in Figure 2 is derived from cables and beams under tension such as risers and casing strings, which have essentially sinusoidal mode shapes. In the last few years a large amount of experimental data have been accumulated on such cylinders, and should be compiled in a separate plot of $2y_{max}/D$ versus S_G without correction factors such as $I^{1/2}/\Psi_{imax}$.

A Proposed Equivalent Response Parameter for Sheared Flow: S_{GE}

Under sheared flow conditions lockin may occur over a limited portion of the cylinder defined by the range X_1 to X_2. For sections of the cylinder outside of this range lockin does not occur and energy is lost due to hydrodynamic damping. In the analysis to follow it is assumed that only one mode has significant response, and even though exciting forces do exist outside of the lockin region they are not at the natural frequency and cause insignificant response. The method proposed is intended to be used to evaluate several possible vibration modes, one at a time, to determine which if any is likely to dominate the response.

A substantial database exists, which tabulates observed response versus the response parameter, S_G, but for uniform flows only. The approach proposed here takes advantage of this existing database by providing an estimate of the response parameter of an equivalent cylinder in a uniform flow, which would behave the same as the cylinder in the sheared flow. In order to be equivalent, both the cylinder in the sheared flow and the equivalent cylinder in the uniform flow must have the following characteristics.

i. The modal response amplitude for each must be the same and therefore from Equation 14

$$\frac{N_{ie}}{\omega_i R_{ie}} = \frac{N_{is}}{\omega_i R_{is}} \quad (42)$$

where the subscripts e and s refer to the equivalent and sheared cases respectively.

ii. The exciting force over the region x_1 to x_2 must be the same for both cases. Outside of this region the forces contributing to lockin are assumed to be zero for the sheared case, and appropriate to that of a fully locked in cylinder in the equivalent case. The equivalent cylinder experiences lockin over its entire length and therefore additional power is fed into the resonant mode outside of the region x_1 to x_2. In order for the response amplitude to stay constant the modal damping in the equivalent cylinder must be increased, so as to dissipate the greater injected power.

Solving for the equivalent damping

$$R_{ie} = R_{is}\,\frac{N_{ie}}{N_{is}} \quad (43)$$

The equivalent response parameter is obtained directly from Equation 26.

$$S_{GE} = \frac{4\pi^2 S_t^2 R_{ie}}{\rho D^2 \omega_i \int_0^L \Psi_i^2(x)\,dx} \quad (44)$$

$$= \frac{8\pi^2 S_t^2 m_e \zeta_{ie}}{\rho D^2} \quad (45)$$

where

$$\zeta_{ie} = \frac{R_{ie}}{2\omega_i M_i} \quad (46)$$

and m_e is defined in Equation 20. It remains to obtain a detailed expression of R_{ie} in terms of R_{is}, and N_{ie}/N_{is}. From Equation 29 and item (ii) above,

$$N_{ie}/N_{is} = \frac{\int_0^L C_L(x)\Psi_i(x)\,dx}{\int_{X_1}^{X_2} C_L(x)\Psi_i(x)\,dx} \cong \frac{P_u}{P_s} \quad (47)$$

and from Equation 5

$$R_{is} = \int_0^L (r_s(x) + r_h(x))\Psi_i^2(x)\,dx \quad (48)$$

where $r_s(x)$ and $r_h(x)$ are the structural and hydrodynamic damping constants per unit length, respectively. For the sake of example, let $r_s(x)$ and $r_h(x)$ be constant everywhere except in the region x_1 to x_2 where $r_h(x)$ the hydrodynamic damping is required to be zero. This leads to

$$R_{is} = (r_s+r_h)\int_0^L \psi_i^2(x)dx - \int_{x_1}^{x_2} r_h \psi_i^2(x)dx \quad (49)$$

Perhaps the most convenient form in which to express S_{GE} is in terms of the S_G for the actual cylinder in a uniform flow.

Therefore from Equations 26, 43, and 44

$$S_{GE} = S_{GU}\frac{R_{ie}}{R_{is}} = S_{GU}\frac{P_u}{P_s}\frac{R_{is}}{R_{iu}} \quad (50)$$

where the subscript u has been added to clarify which quantities come from a uniform flow case and which are due to the sheared conditions. This expression reduces to

$$S_{GE} = \frac{P_u}{P_s}\left[1 + \frac{r_h}{r_s} - \frac{r_h}{r_s}\frac{\int_{x_1}^{x_2}\psi_i^2(x)dx}{\int_0^L \psi_i^2(x)dx}\right]S_{GU} \quad (51)$$

Both the quantity in brackets and the ratio Pu/Ps must always be greater than or equal to one. Therefore S_{GE} is always greater than or equal to S_{Gu}. Note that in the limit as the sheared flow becomes uniform, S_{GE} equals S_{Gu}, as expected.

To proceed farther requires knowledge of $C_L(x)$, the lift coefficient. As an instructive example, but admittedly without experimental justifications, let $C_L(x)$ be proportional to the mode shape $\psi_i(x)$.

$$C_L(x) = C_L\,\psi_i(x) \quad (52)$$

Then the expression for Pu/Ps in Equation 47 simplifies greatly and

$$S_{GE} = \left[\left(1+\frac{r_h}{r_s}\right)\frac{\int_0^L \psi_i^2(x)dx}{\int_{x_1}^{x_2}\psi_i^2(x)dx} - \frac{r_h}{r_s}\right]S_{GU} \quad (53)$$

Continuing the example, assume that the second mode of a cable with the mode shape

$$\psi_2(x) = \sin\frac{2\pi x}{L} \quad (54)$$

is excited over one fourth of its length; x_1=0 to x_2=L/4, as shown in Figure 3. In that case,

$$S_{GE} = \left(4 + \frac{3r_h}{r_s}\right)S_{GU} \quad (55)$$

If the distributed damping per unit length has equal hydrodynamic and material components, then

$$S_{GE} = 7S_{Gu} \quad (56)$$

In this particular example, the cylinder in a sheared flow, with the top quarter of its length experiencing lockin in the second mode, would respond at the same amplitude as the same cylinder in a uniform flow but with a response parameter seven times as great.

Conclusions and Recommendations

If only one mode has a natural frequency excitable by a sheared flow, then a worst case prediction is given by the method described above. However, if two or more modes are potential candidates for resonant lockin excitation then the equivalent response parameter for each should be computed. The mode with the lowest S_{GE} is the most likely lockin candidate. If two or more modes have low S_{GE} values, multimodal non-lockin response or beating between modes may be observed.

The accurate response prediction of flexible cylinders in sheared flows requires much more experimental data. Areas of particular weakness are: i. the current state of knowledge of the hydrodynamic damping on the non-locked in regions of a cylinder; ii. the form of $C_L(x)$ for both uniform and sheared cases; iii. the means of estimating the extent of locked-in regions in sheared flows; iv. the dependence of the locked-in region on damping ratio and bandwidth..

One model for predicting the locked-in region has been offered in the literature (5,6). Experimental observation is needed.

Nomenclature

$C_L(x)$	lift coefficient
D	cylinder diameter
f_s	vortex shedding frequency (Hz)
$H_i(\omega)$	frequency response function or RAO
I_i	mode shape correction factor
K_i	modal stiffness
k_s	reduced damping
L	length of flexible cylinder
M_i	modal mass
m,$m(x)$	constant and variable mass per unit length
m_e	constant m equivalent to a variable m(x)
N_i	modal force
N_{ie}	equivalent system modal force
N_{is}	modal force for sheared case
P_u, P_s	integrals in uniform flow and sheared cases
$q_i(t)$	modal amplitude
R_i	modal damping constant
R_{ie},R_{is}	R_i in equivalent and sheared cases
S_G	response parameter
S_{Gu},S_{GE}	S_G for uniform flow and sheared flow equivalent
S_t	Strouhal number
U	free stream velocity
V_r	reduced velocity
x	longitudinal coordinate
x_1,x_2	range of lockin
$y(x,t)$,$y(x)$	cross flow response amplitude
y_{max}	maximum value of y(x)
δ_s	logarithmic decrement for structural damping
ζ_i	modal damping ratio
ζ_s	structural modal damping ratio
ζ_{ie}	equivalent ζ_i
ω	frequency (radians/sec)
ω_i	natural frequency

ω_s	shedding frequency
ρ	density of water
μ	mass ratio
ϕ_i	phase angle
$\psi_i(x)$	mode shape
ψ_{imax}	maximum value of the mode shape

Acknowledgements

This work was sponsored by the Technology Assessment Research Program of the Minerals Management Service.

References

1. Kim, Y.H., Vandiver, J.K., Holler, R., "Vortex-Induced Vibration and Drag Coefficients of Long Cables Subjected to Sheared Flows," Proceedings of the Fourth International Offshore Mechanics and Arctic Engineering Symposium, Volume One, ASME, Dallas, Texas, Feb. 1985.

2. Griffin, O.M., Ramberg, S.E., "Some Recent Studies of Vortex Shedding with Application to Marine Tubulars and Risers," ASME J. of Energy Resources Technology, Vol. 104, March 1982.

3. Sarpkaya, T., "Vortex-Induced Oscillations, A Selective Review," J. of Applied Mechanics, Vol. 46, June 1979.

4. Griffin O.M., "OTEC Cold Water Pipe Design for Problems Caused by Vortex-Excited Oscillations," Naval Research Laboratory Memorandum Report 4157, March 14, 1980.

5. Griffin, O.M., "Vortex Shedding From Stationary and Vibrating Bluff Bodies in a Shear Flow," Naval Research Laboratory Memorandum Report 4287, August 11, 1980.

6. Stansby, P.K., "The Locking-on of Vortex Shedding Due to the Cross-Stream Vibration of Circular Cylinders in Uniform and Sheared Flows," J. of Fluid Mechanics, Vol. 74, 1976.

7. Griffin, O.M., "Vibrations and Flow-Induced Forces Caused by Vortex Shedding," Symposium on Flow-Induced Vibration, Volume 1, ASME Winter Annual Meeting, Dec. 1984.

8. Botelho, D.L.R., "An Empirical Model for Vortex-Induced Vibrations," Calif. Institute of Tech., Earthquake Engineering Research Laboratory Report No. EERL 82-02, August 1982.

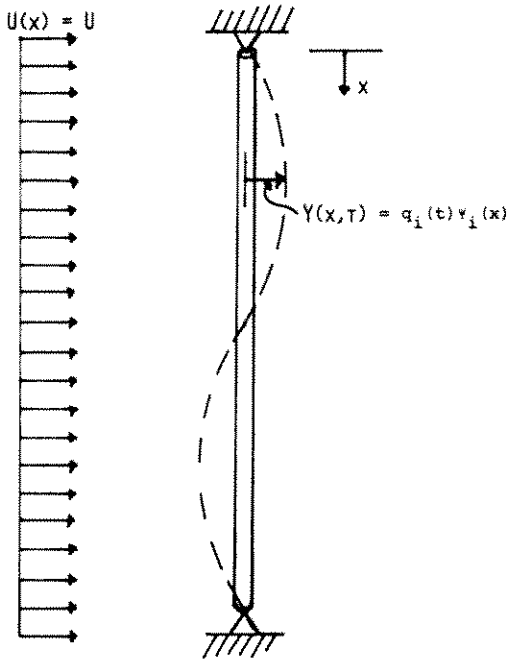

Fig. 1—Flexible cylinder in a uniform flow.

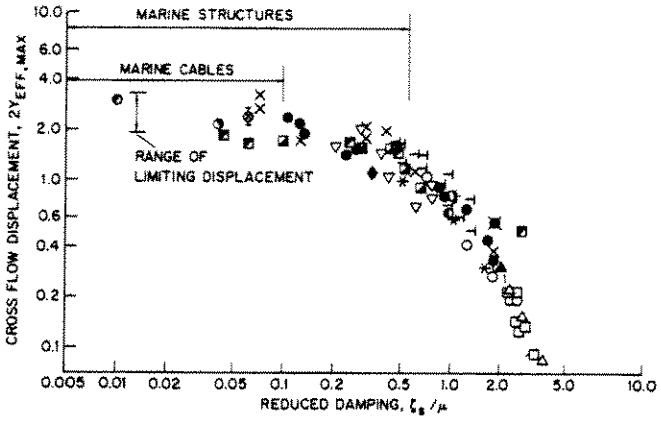

Fig. 2—Response parameter, S_G, vs. $2Y_{eff,max}/D$, from Griffin.[2,4,5,7]

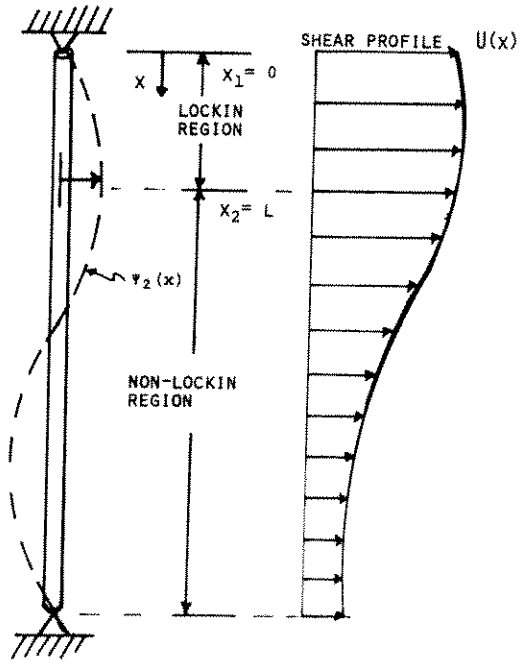

Fig. 3—Second mode partial lockin in a sheared flow.

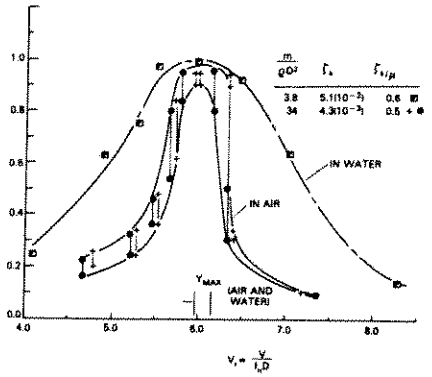

Fig. 4—Reduced velocity vs. $2Y_{max}/D$, from Griffin.[7]

VORTEX-SHEDDING RESPONSE OF LONG CYLINDRICAL STRUCTURES IN SHEAR FLOW

by

E. Wang

Lockheed Advanced Marine Systems

A. K. Whitney

Lockheed Missiles & Space Co., Inc.

K. G. Nikkel†

Lockheed Offshore Systems & Services

ABSTRACT

Lateral vibrations of cylindrical structures caused by vortex shedding in a vertically-sheared cross flow are analyzed. In contrast to the uniform cross flow case, shear flow can excite more than one modal frequency at a time. Thus, the net response of the structure is a superposition of several vibration modes. The amplitude of each mode is determined by a balance between energy fed into the structure over a "locked-on" region of the structure and energy dissipated by fluid damping over the remainder of the structure.

A solution method based on random vibration analysis is developed that uses an empirically-derived lift coefficient and correlation length models. The technique is capable of handling both uniform and sheared (depth-varying) current profiles.

† Retired.

Good quantitative agreement is found between the present method and the very limited field data available for shear flows, although it is concluded that the shear conditions in the tests were not sufficiently strong to validate the theory conclusively. The results show how using uniform-flow approximations to treat shear flow cases can significantly over-predict vibration amplitudes caused by vortex shedding.

INTRODUCTION

Vortex-shedding-induced oscillation of such marine structures as risers, piles, OTEC cold water pipes, and ocean-mining lift pipes, is an important fluid-structure interaction phenomenon because it can lead to accelerated fatigue and increased hydrodynamic loads. Structural damage and even destructive failures can sometimes result.

While a great deal of attention has been focused on this problem, most of the previous work has been devoted, by expediency, to structures in uniform cross flows. The subject has been reviewed recently by King [1], Sarpkaya [2], and Griffin [3,4]. When the approaching free stream is not uniform, one is tempted to use a uniform-flow approximation based, say, on the maximum or average cross-flow velocity. This approach is valid only when the flow variation over the length of the structure is small and when the frequency of any unsteady flow component is small in comparison with the vortex-shedding frequency and the modal frequencies of the structure.

In general, neither of these conditions is satisfied for very long cylindrical structures operating in a typical ocean environment where wind and geostrophic currents cause the cross flow to be both oscillatory and sheared. Fundamental questions concerning the effects of unsteadiness and nonuniformity in the approaching free stream on the formation and shedding of vortices, and on the resulting structural response, remain unanswered.

The purpose of the present work is to investigate the effects of shear in the oncoming flow. Specifically, the cross-flow velocity is assumed to be time-invariant and unidirectional with a magnitude that decreases monotonically with distance below the ocean free surface (see Fig. 1).

A solution technique is developed that is based on the random vibration analysis of

Blevins & Burton [5] (also see Blevins [6]), who investigated flow-induced oscillations in uniform flow. Their method is extended to handle sheared flows as well. The empirically-derived dependence of lift coefficient and correlation length on cylinder amplitude that is part of their analysis is retained. In addition, the present method makes use of the laboratory observations of vortex shedding in shear flows by Mair & Stansby [7] and Stansby [8], which indicate that, despite the continuous spanwise variation in cross flow velocity, vortices are shed in "cells." The shedding frequency jumps discontinuously across cell boundaries.

Based on these observations, the following features of vortex-shedding response of cylindrical structures in shear flow are postulated:

- The structure is divided into vortex-shedding cells. Over each cell the vortex-shedding frequency is locked onto one of the modal frequencies of the structure. The frequency jumps in a stepwise fashion from cell to cell.
- More than one modal frequency of the structure is excited since the frequency of vortex-shedding and the associated lift, or cross-stream force, vary along the length of the pipe.
- Cell boundaries are determined by consideration of the "lock-on" phenomenon which establishes definite limits on the amount by which the local shedding frequency can deviate from the so-called "natural shedding frequency" one would obtain by using the Strouhal number and the local cross-flow velocity.
- For each structural mode excited there is an active region where energy is fed into the structure, and a passive region (the remainder of the pipe) where energy is dissipated, primarily by fluid damping.
- The amplitude of each mode is determined by a balance between energy gained and energy lost for that mode.
- The total structural response is obtained as a sum-of-squares superposition of all of the vibration modes excited.

These features have been incorporated into a math model and computer code that calculates structural response amplitude and bending stress as a function of spanwise location for long cylindrical structures exposed to arbitrary current profiles.

Comparisons show that the present technique agrees well with a data correlation of both field and laboratory test data for the case of uniform flow. Results are generated showing the vortex-shedding-induced response of typical 500 to 5000 ft production and drilling risers operating in sheared currents that range from nearly zero to those that can be expected in the Gulf Stream. These data clearly show that use of typical uniform-flow approximations to sheared current profiles can significantly over-predict the effects of vortex shedding.

Comparison is also made between the present predictions and test data for a model pile in shear flow. Good agreement is found for the maximum pile response, although the velocity range for excitation is under-predicted. It is concluded the test conditions were not suitable to verify the effect of shear flow conclusively.

VORTEX SHEDDING FORCES

In the range of cross-flow velocities and diameters of practical interest, flow past a cylindrical body is characterized by the alternate shedding of vortices forming a "Karman vortex street" in the wake of the structure. The vortex shedding generates periodic, or quasi-periodic, lift and drag forces. The lift-force frequency is the same as the frequency of one complete cycle of the vortex shedding. The unsteady drag frequency has twice this frequency. The drag force is an order of magnitude smaller than the lift force.

Although the cylinder is a two-dimensional shape, the flow past it is three-dimensional because vortex shedding is not fully correlated along the span. A measure of the average length over which the shedding is correlated is the correlation length, ℓ_c. For stationary cylinders, $\ell_c \simeq 2.5D$ to $5D$.

A nondimensional parameter that governs the flow regime is the Reynolds number, $Re = VD/\nu$, where V is the cross-flow velocity (which may be depth-dependent). D is the structure outer diameter, and ν is the kinematic viscosity of seawater. For stationary

cylinders, the vortex-shedding frequency, f_s, is nearly proportional to V in the subcritical Re-regime, $2 \times 10^2 < Re < 3 \times 10^5$. Therefore the reduced frequency, or Strouhal number S, given by

$$S = f_s D/V \tag{1}$$

is nearly constant, $S \simeq 0.20$, in this Re range. In the critical Re-regime, $3 \times 10^5 < Re < 3.5 \times 10^6$, the viscous boundary layer becomes turbulent upstream of the separation points and the wake is more disorganized. Strouhal numbers from 0.20 to 0.40 have been reported by Jones, *et al* [9]. For $Re > 3.5 \times 10^6$, the turbulent vortex street is re-established [6], and $S \simeq 0.30$.

If the cylinder is part of a lightly-damped structure, and if the shedding frequency, f_s, is near a modal frequency of the structure, f_n, lateral oscillations may occur. Parameters that govern the susceptibility of a structure to vortex-shedding-induced oscillations are the reduced velocity, V_{rn}, and the reduced damping, δ_{rn}, given by

$$V_{rn} = V/f_n D \tag{2}$$

and

$$\delta_{rn} = 4\pi\zeta_n m/\rho D^2 \tag{3}$$

Here m is the mass per unit length of the cylinder (including internal fluid mass and the added mass of the surrounding seawater), ζ_n is the damping coefficient of the nth vibration mode, and ρ is the seawater density. The subscripts n mean that these parameters are associated with the nth mode.

For lightly damped structures ($\delta_{rn} \leq 10$), oscillations can occur in a range of $4.5 < V_{rn} < 10.0$, with a peak response at about $V_{rn} = 7.25$.

Lateral oscillations of a cylinder at, or near, the "natural" shedding frequency, $f_s = SV/D$, increase the vortex strength, the lift and drag forces, and the correlation length. In addition, the vortex shedding frequency may lock onto a structural vibration frequency. All of these effects are found to depend on the lateral vibration amplitude, A_y.

The lift coefficient, $C_L = \tilde{L}/\frac{1}{2}\rho V^2 D$, where $\tilde{L}$ is the unsteady lift force per unit length of the cylinder, is found to increase from about 0.4 at $A_y/D = 0$ to about 0.5 at $A_y/D = 0.4$, and then decreases to zero at $A_y/D = 1.5$. The lift force referred to is that component of the force in-phase with the transverse cylinder velocity. The correlation length increases rapidly from about $3.5D$ to $40D$ as A_y/D increases from zero to 0.1 in the subcritical case, and from $2.5D$ to $10D$ for the supercritical case.

SOLUTION METHOD

The solution method is an extension of the random vibration approach developed by Blevins & Burton [5] for the uniform-current case.

As a typical cylindrical marine structure, we consider the riser configuration shown in Fig. 1, with the top of the riser at $z = 0$, the mean waterline at $z = h$, and the bottom of the riser at $z = L$. The current $V(z)$ is directed along the positive x-axis. Unsteady lift forces attributable to vortex shedding cause the structure to oscillate in the cross-flow direction, or the $\pm y$-direction.

Random Vibration Analysis

The mean-square displacement of the structure is given by

$$\overline{y^2(z,t)} = \sum \overline{q_n^2(t)}\psi_n^2(z) + \Delta \tag{4}$$

where $\psi_n(z)$ is the nth mode shape function of the structure, Δ is a small error caused by cross-correlation, and

$$\overline{q_n^2(t)} = \int_0^\infty F(\omega/q_n^2)\, d\omega \tag{5}$$

is the mean-square Lagrangian coefficient evaluated by integrating the following power spectral density (PSD):

$$F(\omega/q_n^2) = \frac{\int_h^L \int_h^L \psi_n(z)\psi_n(z')F(\omega/L(z)L(z'))\, dz\, dz'}{\left|Z_n(i\omega)\right|^2 \left[\int_0^L m(z)\psi_n^2(z)\, dz\right]^2} \tag{6}$$

Here $Z_n(i\omega)$ is the impedance of the nth mode

$$Z_n(i\omega) = -\omega^2 + 2i\varsigma_n\omega\omega_n + \omega_n^2 \tag{7}$$

ω_n is the nth modal frequency (rad/sec), and ζ_n is the damping coefficient of the nth mode.

The cross-correlation PSD function is assumed to have the form

$$\begin{aligned} F(\omega/L(z)L(z')) = &\frac{1}{B\omega_s\sqrt{\pi}} \\ &\times \left\{ \tfrac{1}{2}\rho V^2(z) C_L(z) \exp[-(1-\omega/\omega_s)^2/2B^2] \right. \\ &\times \tfrac{1}{2}\rho V^2(z') C_L(z') \exp[-(1-\omega/\omega_s')^2/2B^2] \\ &\left. \times \exp[-2|z-z'|/\ell_c] \operatorname{sgn}(\psi_n(z)\psi_n(z')) \right\} \end{aligned} \tag{8}$$

where B is the vortex shedding frequency bandwidth and ω_s is the shedding frequency (a function of z). As mentioned in the Introduction, the shedding frequency is assumed to lock onto the modal frequency ω_n over a certain region of the cylinder, $z_{n,min} < z < z_{n,max}$, which will be denoted by R_n. The method of allocating lock-on regions is described below.

If the vortex shedding bandwidth, B, is comparable in width to the response bandwidth of the oscillator, ζ_n, it is possible to show that the maximum response amplitude of mode n is

$$\begin{aligned} \left(\frac{A_n}{D}\right)^2 &= \left(\frac{\rho\psi_{n,max}}{4\zeta_n\omega_n^2}\right)^2 \int_{R_n}\int_{R_n} f(z)\, f(z')\, e^{-2|z-z'|/\ell_c}\, dz\, dz' \\ f(z) &= V^2(z)\,|\psi_n(z)|\,K_1 K_2\, C_L(z) \end{aligned} \tag{9}$$

The constant K_1 is a function of the bandwidth of the oscillator; K_2 relates the root-mean-square (RMS) amplitude to the maximum amplitude. The constants K_1 and K_2 and the lift coefficient C_L have been found empirically by Blevins & Burton [5] to satisfy

$$\begin{aligned} K_1 K_2 C_L(z) = &a + b\left(\frac{A_n}{D}\right)\left(\frac{\psi_n(z)}{\psi_{n,max}}\right) + c\left(\frac{A_n}{D}\right)^2\left(\frac{\psi_n(z)}{\psi_{n,max}}\right)^2 \\ &a = 0.35, \quad b = 0.60, \quad c = -0.93 \end{aligned} \tag{10}$$

For the correlation length, the same authors propose

$$\ell_c/D = \begin{cases} 5 + \dfrac{100(A_n/D)}{0.5 - (A_n/D)} & \text{for } A_n/D < 0.5 \\ \infty & \text{for } A_n/D \geq 0.5 \end{cases} \tag{11}$$

Since both C_L and ℓ_c depend on A_n/D, Eq. (9) must be solved iteratively for the unknown amplitude, A_n/D.

Once the amplitude of each mode is determined in this manner the total response amplitude $A(z)$ is given by a sum-of-squares superposition:

$$\frac{A(z)}{D} = \left\{ \sum_n \left(\frac{A_n}{D} \right)^2 \left(\frac{\psi_n(z)}{\psi_{n,max}} \right)^2 \right\}^{1/2} \tag{12}$$

Allocation of Lock-On Regions

Observations of lightly damped cylindrical structures in uniform cross flow indicate that the vortex shedding frequency will lock on a structural natural frequency over the reduced velocity range

$$4.5 \leq V_{rn} \leq 10 \tag{13}$$

with a peak response at about $V_{rn} = 7.25$. If one applies these results to a sheared current profile, then the range of current velocities over which the structure will be excited by a shedding frequency f_n is given by

$$\begin{aligned} V(z) &\geq V_{n,min} \equiv 4.5 f_n D \\ V(z) &\leq V_{n,max} \equiv 10.0 f_n D \end{aligned} \tag{14}$$

with a peak excitation at $V_{n,peak} = 7.25 f_n D$. For a given current profile these inequalities determine the lock-on range for the nth mode (see Fig. 2).

The mode allocation scheme is as follows: Starting at the upper end of the structure where the current velocity is the highest, the mode with $V_{n,peak}$ closest to the upper current velocity is selected for the upper cell. Its upper boundary is $z = h$, while the lower boundary corresponds to that depth at which $V_{n,min} = V(z)$. The mode excited at the next cell is the highest mode with a value of $V_{n,peak}$ that is less than $V_{n,min}$ corresponding to the lower limit of the upper cell. The lower limit for this cell is again found at the location where the current velocity equals $V_{n,min}$ for this mode. This process is continued down the entire length until all portions of the structure have been allocated.

Depending on the spacing of the modal frequencies of the structure, and the particular current profile, some portions of the cylinder may not be excited by any of the modal frequencies. As currently structured, the mode allocation scheme does not allow one cell to incur into another, nor does it allow gaps between adjacent cells. In this respect, it appears that the allocation scheme is conservative in that the highest possible mode for a particular cell is always selected. Several variations of this scheme were tested. All of them resulted in essentially the same structural responses.

In reality, the allocation of vortex shedding cells along the structure probably depends on the time evolution of the flow field, thus making it difficult to choose a single algorithm that will apply to all cases. This part of the model would obviously benefit the most by comparison with experimental data.

Fluid Damping

A linearized formulation is used to account for fluid damping over the non-locked-on region of the structure. This approach is valid as long as the cross-flow velocity is large in comparison to the lateral cylinder velocity.

The drag force per unit length is given by

$$\vec{F}_D = \tfrac{1}{2}\rho D C_D |\vec{V}_R| \vec{V}_R \tag{15}$$

where $\vec{V}_R = (V(z), -\partial y/\partial t)$ is the relative flow velocity. For $|\partial y/\partial t| \ll V$, the component of $\vec{F}_D$ in the lateral direction is

$$F_y \simeq -\tfrac{1}{2}\rho D C_D V(z) \frac{\partial y}{\partial t} \tag{16}$$

In order to estimate an equivalent damping coefficient for the structure, we temporarily revert to a deterministic formulation. The force acting on the structure is composed of a vortex-shedding force over the lock-on region R_n and the damping force Eq. (16) over the remainder of the structure $L - R_n$, so that the lift force per unit length is given by

$$L(z,t) = \begin{cases} \tfrac{1}{2}\rho D V^2 C_L e^{i\omega_n t} & \text{for } z \in R_n \\ -\tfrac{1}{2}\rho D C_D V \dfrac{\partial y}{\partial t} & \text{for } z \in L - R_n \end{cases} \tag{17}$$

Let the displacement $y(z,t)$ be expanded in normal modes as

$$y(z,t) = \sum_n q_n(t)\,\psi_n(z) \tag{18}$$

Then the equation of motion for the nth mode is

$$\begin{aligned} &\ddot{q}_n + 2\zeta\omega_n\dot{q}_n + \omega_n^2 q_n \\ &\qquad = \int_0^L L(z,t)\psi_n(z)\,dz \Big/ \int_0^L m\psi_n^2(z)\,dz \end{aligned} \tag{19}$$

where the damping coefficient ζ accounts for internal material dissipation only. After substituting from Eq. (17) for $L(z,t)$ there results

$$\begin{aligned} &\ddot{q}_n + 2\zeta_n\omega_n\dot{q}_n + \omega_n^2 q_n \\ &\qquad = \int_{R_n} \tfrac{1}{2}\rho D V^2 C_L e^{i\omega_n t}\psi_n(z)\,dz \Big/ \int_0^L m\psi_n^2\,dz \end{aligned} \tag{20}$$

where the damping coefficient ζ_n is given by

$$\zeta_n = \zeta + \frac{\rho D C_D}{4\omega_n} \int_{L-R_n} V\psi_n^2\,dz \Big/ \int_0^L m\psi_n^2\,dz \tag{21}$$

This expression for damping coefficient is used in Eq. (9) to determine the modal amplitude.

Bending Stress

In the deterministic case, pipe bending stress is given by

$$\sigma = \tfrac{1}{2} E D_o \frac{\partial^2 y}{\partial z^2} \tag{22}$$

where E is Young's modulus and D_o is the OD of the structural pipe (OD of structure minus twice the buoyancy thickness, if present). The corresponding expression for bending stress amplitude in the random case is found by using Eq. (12) to evaluate the mean-square second derivative of the pipe displacement. The final result is

$$\sigma(z) = \tfrac{1}{2} E D D_o \left\{ \sum \left(\frac{A_n}{D}\right)^2 \left(\frac{\psi_n''(z)}{\psi_{n,max}}\right)^2 \right\}^{1/2} \tag{23}$$

where the primes denote differentiation with respect to z.

RESULTS AND DISCUSSION

A computer program was written to implement the preceding theory. The program utilizes an existing finite-difference code and eigen-processor that calculate mass and stiffness matrices and eigen-modes and frequencies.

In order to compare the results of the present theory with existing methods, a series of computer runs were made for typical riser configurations. Both drilling and production risers were studied in water depths of 500, 1500, and 5000 ft. The riser properties are listed in Table 1.

Comparisons are made between the present theory and a data correlation technique that was developed specifically for uniform cross flows, although it can be applied to sheared profiles by using either the average or the maximum of the profile.

Uniform Cross Flow Case

For the purpose of checking out the present technique, it was first compared with a data correlation technique for the case of uniform cross flow. Iwan & Blevins [10] have shown that the following expression for maximum amplitude agrees well with test data for a variety of cylindrical structures:

$$\frac{A_n}{D} = \frac{0.07\gamma_n}{(\delta_{rn}+1.9)S^2}\left[0.30+\frac{0.72}{(\delta_{rn}+1.9)S}\right]^{1/2} \tag{24}$$

Here δ_{rn} is the reduced damping (see Eq. (3)) and γ_n is a mode shape factor defined by

$$\gamma_n = \psi_{n,max}\left[\int_0^L \psi_n^2(z)\,dz \Big/ \int_0^L \psi_n^4(z)\,dz\right]^{1/2} \tag{25}$$

This expression applies over a range of reduced velocities given by inequality (13). If the modal frequency spacing is small enough, more than one mode may be excited for a particular (uniform) cross flow velocity. Since there are no criteria for deciding which mode is excited, a range of displacements and bending stresses for all of the modes that are capable of being excited according to Eq. (13) are presented.

Comparisons of the data correlation method and the random vibration results are shown in Tables 2 and 3 for uniform velocity profiles of 4.22 ft/sec (2.5 knots) and 6.76

ft/sec (4.0 knots), respectively. The results indicate that the two techniques predict nearly the same amplitudes with the random vibration amplitudes averaging about nine percent below the data correlation displacements. The bending stresses obtained by the random vibration method are also in fairly good agreement with the lower range of bending stresses predicted by the data correlation method. Results for the 1500-ft and 5000-ft are not presented for the higher velocity case because this velocity excites modes that are beyond the computational range of the particular eigen-processor that is presently used to find mode shapes.

Sheared Cross Flow Case

Results are next presented for the case of sheared cross flow which is more typical of the actual ocean environment.

A detailed illustration of the application of the present random vibration method is shown in Figs. 3(a)–(b). In this example a 1500-ft drilling riser is subjected to the sheared velocity profile shown in Fig. 3(a). The same Figure shows how excited modes are allocated along the length of the structure. In this case, three modes are excited with lock-on regions denoted by the R's to the right of Fig. 3(a).

It should be noted that while each of the three modes is excited only over a subregion of the structure, the response to the excitation extends over the entire pipe. Fig. 3(b) shows the mode shapes that are excited by the vortex shedding with the actual amplitudes that are obtained by solving Eq. (9). The final step is to superimpose the individual modal responses according to Eq. (12). The result of this sum-of-squares superposition is show in Fig. 3(c).

The remainder of the shear flow cases are for the two velocity profiles shown in Fig. 4. Profile 1 is piecewise linear with the highest shear occurring at the water surface, while profile 2 has uniform shear.

While the data correlation technique was developed for uniform cross flows, it is tempting to apply it to shear flows by using an equivalent uniform velocity based either on the average velocity or the maximum velocity. This idea is tested in the last series of

results which compare the data correlation and random vibration methods when both are applied to shear flows.

Tables 4 and 5 show such a comparison for current profile 1. The data correlation results in Table 4 are based on the average current velocity, while those in Table 5 are based on the maximum velocity. Displacements obtained by the random vibration method average about forty percent lower than those given by the data correlation method. A similar trend is found for bending stresses, although now the discrepancy is greater. When the data correlation method is based on the average velocity, the agreement with random vibration technique is fairly close. However, use of the maximum velocity with the data correlation method clearly over-predicts the bending stress when compared to random vibration results.

A similar trend is shown in Tables 6 and 7 for current profile 2. Here again use of the average velocity, rather than the maximum velocity, in the data correlation method, gives closer agreement with the random vibration results.

Discussion of Cognac Model Tests

One of the few instances of shear-flow test data available in the open literature is from model tests of foundation piles for Shell's Cognac platform (e.g., see Fischer, *et al* [11]). Vortex shedding effects were of concern here both during "stabbing" of the pile, when the pile is suspended by cables in a double pendulum configuration, and after installation of the pile when it behaves like a cantilevered beam. A series of scale model tests were made of the pile in both uniform and sheared profiles. The shear profile was nearly linear; the velocity at the bottom was 60% that at the top.

Both the data correlation and random-vibration methods were applied to find pile response in the "stabbed" configuration. Figure 5 shows a comparison of these methods with the experimental data. Here the nondimensional tip amplitude is plotted against the reduced velocity based on surface velocity, pile diameter, and first modal frequency. The data correlation technique is seen to over-predict the data by about 20%. Better agreement is found with the random vibration method, although the predicted range of excitation is

shifted to lower velocities.

Another test series was run with the cantilevered pile during the driving operation. An mass was placed at the end of the pile to simulate the hammer. Both smooth and rough hammers with three different densities were tested; comparisons are made with the data for a smooth hammer with specific gravity of 1.5. The nondimensional amplitude versus reduced velocity for this case are shown in Fig. 6.

Fairly good agreement is again found for the maximum response with the random vibration technique, while the data correlation method over-predicts by 140%. The wide range of response velocities is not reproduced by the random vibration results; investigations are currently being made of the sensitivity of the solution to the lift-force and correlation-length parameters that occur in Eqs. 10 and 11.

For the effects of shear flow to be important it is necessary that either the modal spacing be dense enough, or the shear profile be high enough, to excite more than one mode. In the present case the ratio of second to first modal frequencies is about 6, while the current profile only increases by a factor of 1.8 in going from the the bottom to the top of the pile. This being the case, one would not expect the second mode to be excited at all under the conditions of the tests. This is confirmed by the results of the random vibration analysis.

In summary, the Cognac model tests are probably not a critical indicator of the effects of shear flow on vortex shedding response of structures. Further tests involving structures with more closely spaced modal frequencies in more highly sheared flows are required.

CONCLUSIONS

A random vibration model and accompanying computer program have been developed to calculate the response of structures in sheared cross flows. The model predicts that more than one modal frequency can be excited in shear flows, but that the number of modes excited and their lock-on ranges depend on the distribution of modal frequencies and on the particular velocity profile.

Comparisons of the present method with a data correlation technique show good agree-

ment for the case of uniform cross flow. The data correlation results tend to over-predict displacements and bending stress for the case of shear flow, although better agreement is obtained if one bases the reference velocity used in data correlation technique on the average cross flow velocity rather than the maximum velocity.

Further experiments are required to verify the effects of shear flow on vortex shedding response of structures.

NOMENCLATURE

$A(z)$	Riser amplitude
A_n	Amplitude of the nth mode
B	Bandwidth of unsteady lift force
C_D	Drag coefficient
C_L	Unsteady lift coefficient
D	Outer diameter of cylinder
E	Young's modulus
f_n	Modal frequency
f_s	Shedding frequency
$F(\omega/-)$	Power spectral density
$\vec{F}_D$	Drag force
F_y	Lateral force component
h	Waterline location
K_1, K_2	Constants
ℓ_c	Correlation length
L	Cylinder length
$\tilde{L}$	Unsteady lift force
m	Cylinder mass per unit length
n	Mode number
q_n	Lagrangian coefficient
R_n	Lock-on region

Re	Reynolds number
S	Strouhal number
t	Time
$V(z)$	Cross flow velocity
$\vec{V}_R$	Relative velocity
V_{rn}	Reduced velocity
x	Streamwise coordinate
y	Lateral coordinate
$y(z,t)$	Lateral displacement
z	Coordinate along cylinder axis
Z_n	Impedence of nth mode
γ_n	Mode shape factor
δ_{rn}	Reduced damping
Δ	Cross-correlation error
ς, ς_n	Damping coefficients
ν	Kinematic viscosity
ρ	Seawater density
σ	Bending stress
$\psi_n(z)$	Mode shape
ω_n	Modal frequency (rad/sec)
ω_s	Shedding frequency (rad/sec)

REFERENCES

1. King, R., "A Review of Vortex Shedding Research and Its Applications," *Ocean Engng.*, **4**, p. 141, Pergamon Press, 1977.
2. Sarpkaya, T., "Vortex-Induced Oscillations," *J. Appl. Mech.*, **46**, p. 241, 1979.
3. Griffin, O. M., "Vortex Excited Oscillations of Marine Structures with Application to the OTEC Cold Water Pipe," *6th OTEC Conf.*, Washington, D.C., June, 1979.
4. Griffin, O. M., "OTEC Cold Water Pipe Design for Problems Caused by Vortex-

Excited Oscillations," *Ocean Engng.*, **8**, p. 129, Pergamon Press, 1981.

5. Blevins, R. D., and T. E. Burton, "Fluid Forces Induced by Vortex Shedding," *J. Fluid Eng.*, **98**, p. 19, 1976.
6. Blevins, R. D., *Flow-Induced Vibration*, Van Nostrand, New York, 1977.
7. Mair, W. A., and P. K. Stansby, "Vortex Wakes of Bluff Cylinders in Shear Flow," *SIAM J. Appl. Math.*, **28**, p. 519, 1975.
8. Stansby, P. K., "The Locking-On of Vortex Shedding Due to the Cross-Stream Vibration of Circular Cylinders in Uniform and Shear Flows," *J. Fluid Mech.*, **74**, p. 641, 1976.
9. Jones, G. W., Jr., J. J. Concotta, and R. W. Walker, "Aerodynamic Forces on a Stationary and Oscillating Circular Cylinder at High Reynolds Number," NASA TR R-300, Feb., 1969.
10. Iwan, W. D., and R. D. Blevins, "A Model for the Vortex-Induced Oscillation of Structures," *J. Appld. Mechs.*, **44**, p. 581, 1974.
11. Fischer, F. J., W. T. Jones, and R. King, "Current-Induced Oscillations of Cognac Piles During Installation – Prediction and Measurement," *Proc. Symp. on Practical Experiences with Flow-Induced Vibrations*, Karlsruhe, p. 570, Sept., 1979.

Table 1
RISER PHYSICAL PROPERTIES

PROPERTY	WATER DEPTH		
	500 ft	1500 ft	5000 ft
Drilling Riser			
Piper OD (in)	21	21	21
Pipe wall (in)	0.625	0.625	0.625
Buoyancy wall (in)	none	42	42
Buoyancy weight (pcf)	none	30	30
Mud weight (lb/gal)	12	12	12
Wet weight (lb/ft)	214	10.97	10.97
Top tension (kips)	400	500	1000
Production Riser			
Pipe OD (in)	9.625	9.625	9.625
Pipe wall (in)	0.625	0.625	0.625
Mud weight (lb/gal)	8.6	8.6	8.6
Wet weight (lb/ft)	60	60	60
Top tension (kips)	100	200	400

Table 2
COMPARISON OF DATA CORRELATION & RANDOM VIBRATION
FOR A UNIFORM CURRENT OF 4.22 FT/SEC

RISER	PEAK AMPLITUDE (ft)		PEAK BENDING STRESS (psi)	
	DATA CORRELATION	RANDOM VIBRATION	DATA CORRELATION	RANDOM VIBRATION
500 ft Drilling	2.28	2.09	8575-19102	7813
1500 ft Drilling	4.71	4.28	4843-19135	4390
5000 ft Drilling	4.71	4.32	3447-11662	3924
500 ft Production	1.16	0.96	8049-17431	6609
1500 ft Production	1.18	0.97	4647-7131	4748
5000 ft Production	1.27	1.08	4831-10737	4711

Table 3
COMPARISON OF DATA CORRELATION & RANDOM VIBRATION
FOR A UNIFORM CURRENT OF 6.76 FT/SEC

RISER	PEAK AMPLITUDE (ft)		PEAK BENDING STRESS (psi)	
	DATA CORRELATION	RANDOM VIBRATION	DATA CORRELATION	RANDOM VIBRATION
500 ft Drilling	2.28	2.07	19102-33288	12988
1500 ft Drilling	4.70	4.23	13405-42224	17248
5000 ft Drilling	4.70	4.30	7547-29758	10668
500 ft Production	1.19	0.97	12338-30244	12959

Table 4
COMPARISON OF DATA CORRELATION* & RANDOM VIBRATION
FOR SHEAR FLOW CURRENT PROFILE #1

RISER	PEAK AMPLITUDE (ft)		PEAK BENDING STRESS (psi)	
	DATA CORRELATION	RANDOM VIBRATION	DATA CORRELATION	RANDOM VIBRATION
500 ft Drilling	2.27	1.64	2021	1508
1500 ft Drilling	4.68	3.99	508	1198
5000 ft Drilling	4.73	2.05	853	336
500 ft Production	1.17	0.57	2011	1242
1500 ft Production	1.20	0.77	644-1843	1169
5000 ft Production	1.27	0.75	4831-10737	3271

* Uniform flow velocity based on average velocity

Table 5
COMPARISON OF DATA CORRELATION* & RANDOM VIBRATION
FOR SHEAR FLOW CURRENT PROFILE #1

RISER	PEAK AMPLITUDE (ft)		PEAK BENDING STRESS (psi)	
	DATA CORRELATION	RANDOM VIBRATION	DATA CORRELATION	RANDOM VIBRATION
500 ft Drilling	2.28	1.64	8575-19102	1508
1500 ft Drilling	4.71	3.99	4843-19135	1198
5000 ft Drilling	4.71	2.05	3447-11662	336
500 ft Production	1.16	0.57	8049-17431	1242
1500 ft Production	1.18	0.77	4647-7131	1169
5000 ft Production	1.27	0.75	4831-10737	3271

* Uniform flow velocity based on maximum velocity

Table 6
COMPARISON OF DATA CORRELATION* & RANDOM VIBRATION
FOR SHEAR FLOW CURRENT PROFILE #2

RISER	PEAK AMPLITUDE (ft)		PEAK BENDING STRESS (psi)	
	DATA CORRELATION	RANDOM VIBRATION	DATA CORRELATION	RANDOM VIBRATION
500 ft Drilling	2.28	1.75	8575-19102	12732
1500 ft Drilling	4.70	3.15	4843-19135	12434
5000 ft Drilling	4.72	3.24	3446-11662	8038
500 ft Production	1.16	0.72	8049-17431	10765
1500 ft Production	1.18	0.76	4647-7131	4594
5000 ft Production	1.27	0.75	4831-10737	3270

* Uniform flow velocity based on average velocity

Table 7
COMPARISON OF DATA CORRELATION* & RANDOM VIBRATION
FOR SHEAR FLOW CURRENT PROFILE #2

RISER	PEAK AMPLITUDE (ft)		PEAK BENDING STRESS (psi)	
	DATA CORRELATION	RANDOM VIBRATION	DATA CORRELATION	RANDOM VIBRATION
500 ft Drilling	2.28	1.75	19102-33288	12732
1500 ft Drilling	4.70	3.15	13405-42224	12434
5000 ft Drilling	4.70	3.24	7547-29758	8038
500 ft Production	1.19	0.72	12338-30244	10765

* Uniform flow velocity based on maximum velocity

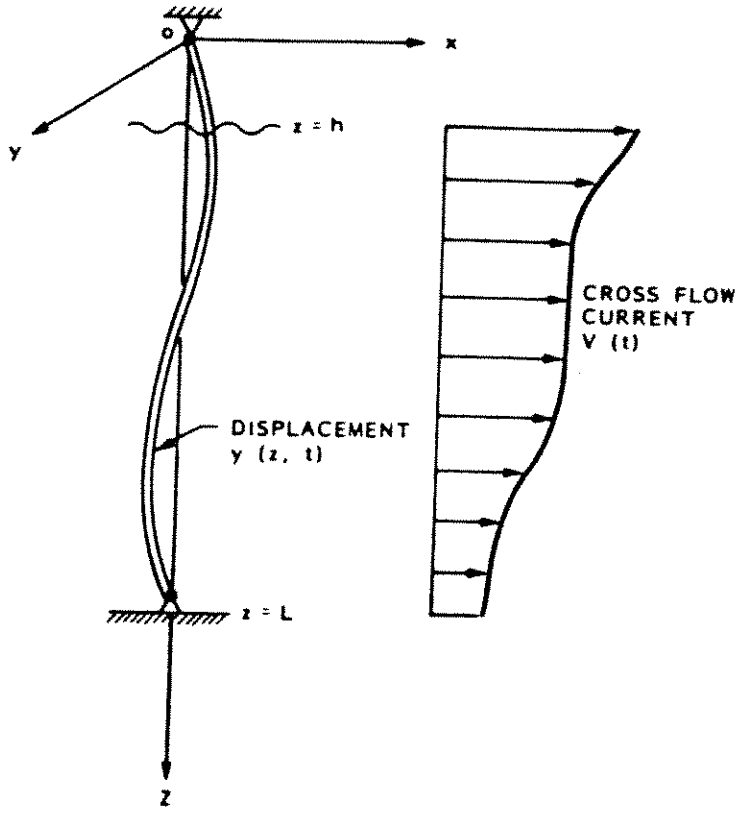

Fig. 1 Riser in Sheared Crossflow.

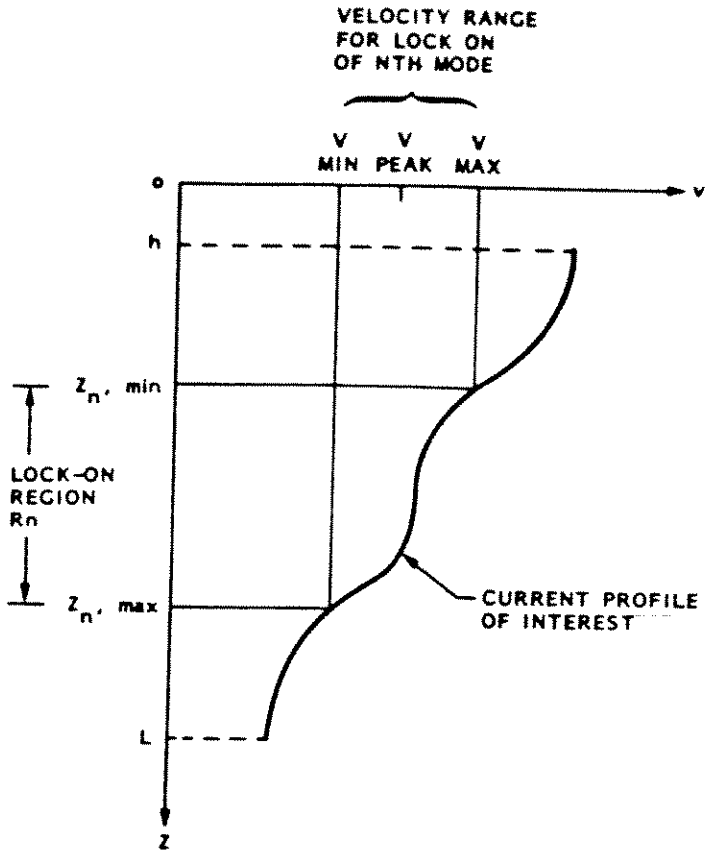

Fig. 2 Determination of Lock-on Region for the *n*th Mode.

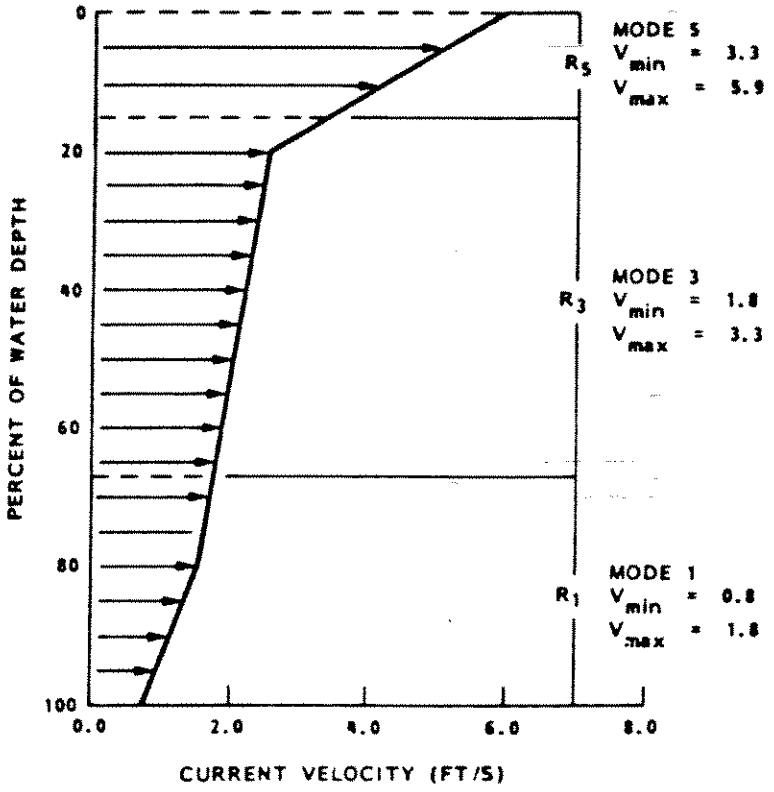

Fig. 3a Example of Mode Allocation Scheme.

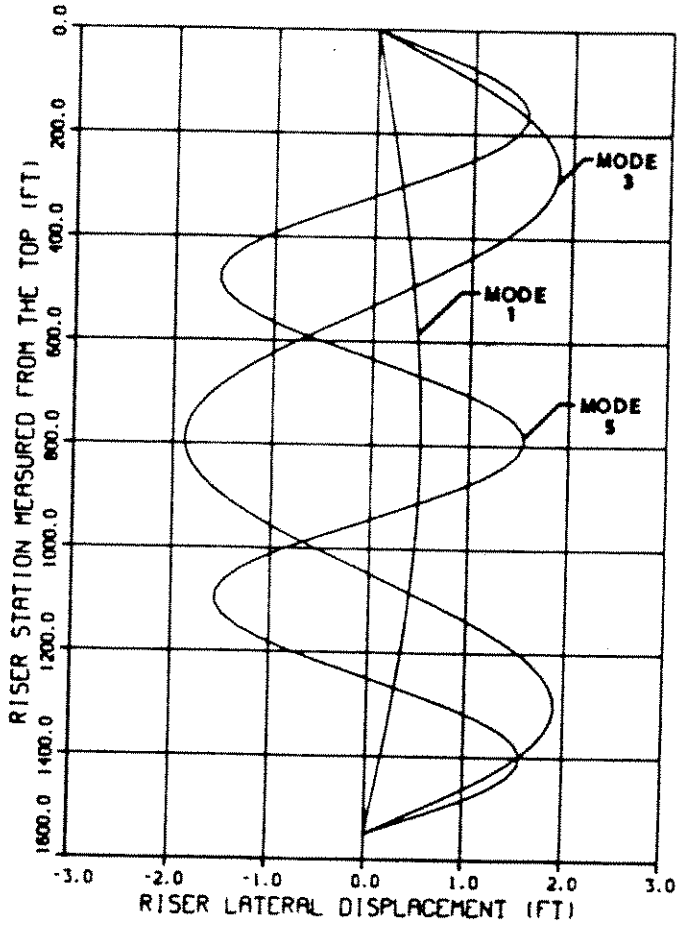

Fig. 3b Mode Shapes Excited.

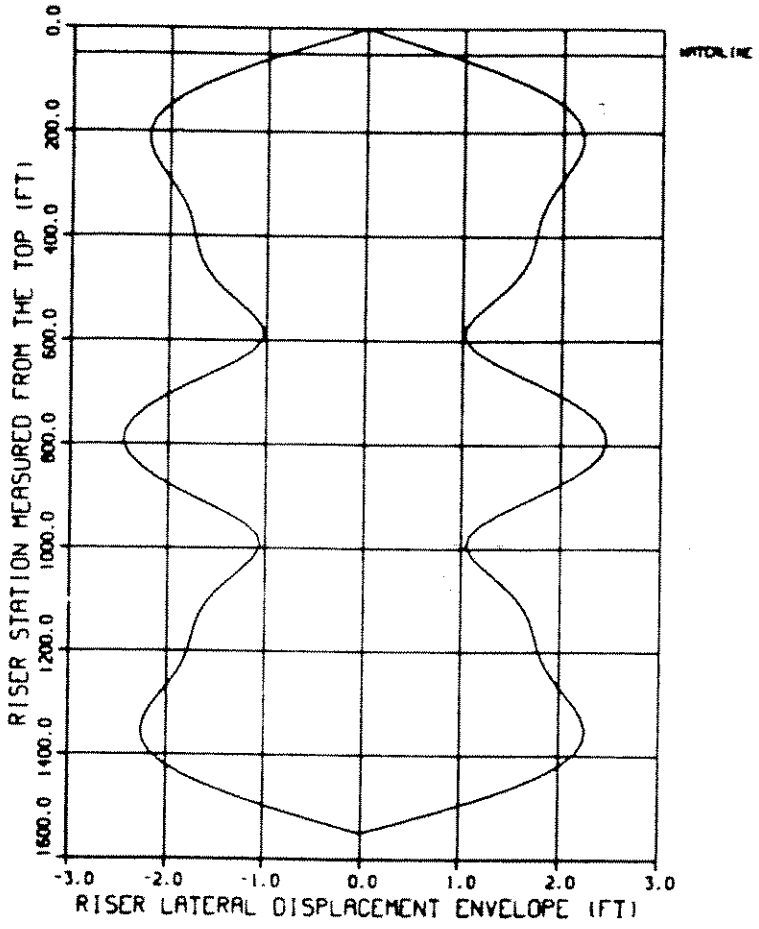

Fig. 3c Total Riser Response Envelope.

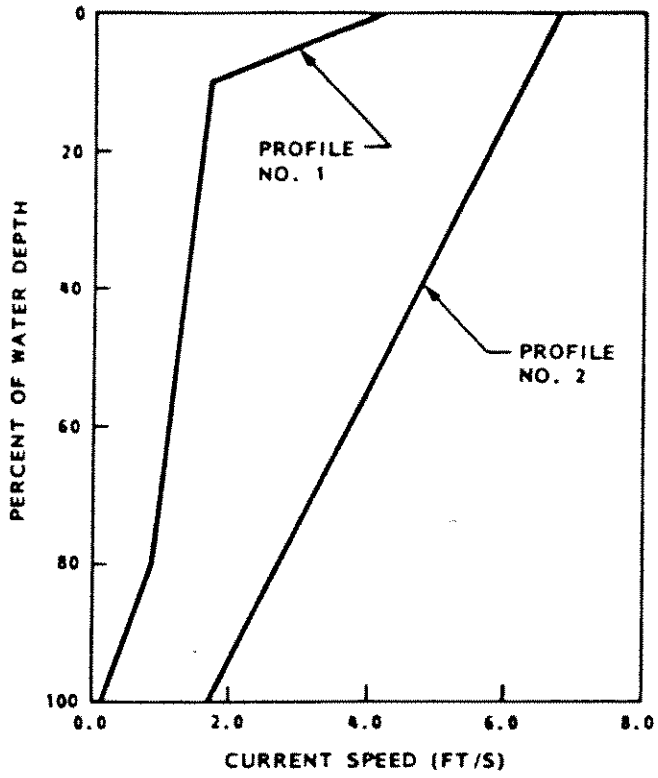

Fig. 4 Current Profiles Used in Riser Response Calculations.

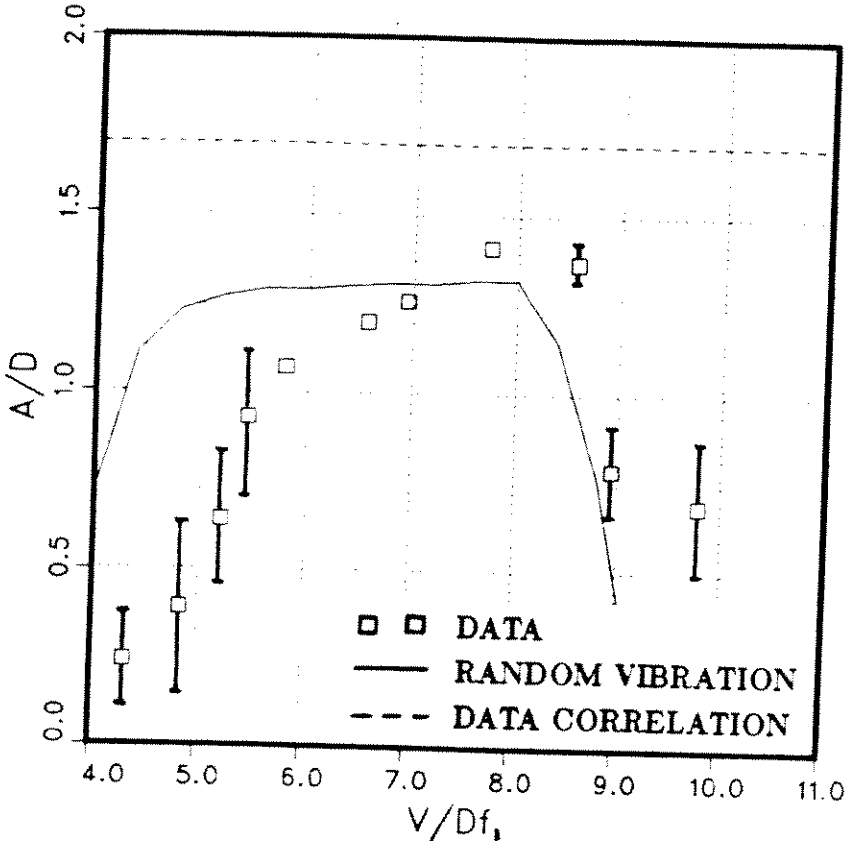

Fig. 5 Comparison of Theory and Data for the Bare Pile Model.

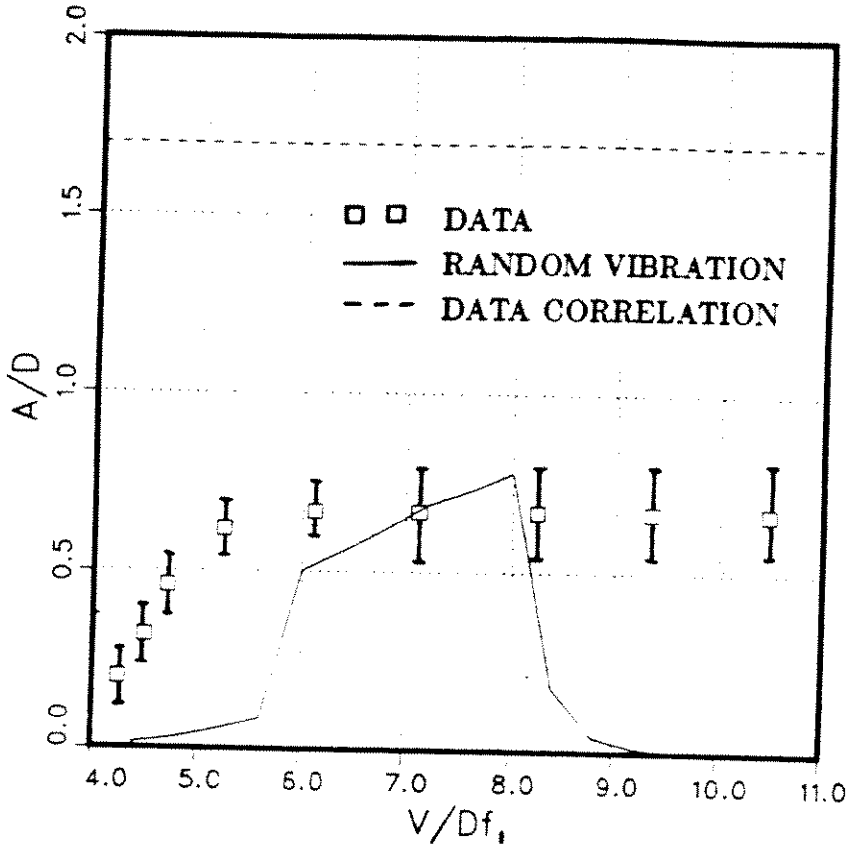

Fig. 6 Comparison of Theory and Data for the Pile Model with Hammer.